

## Corrosion Inhibition and Adsorption Characteristics of Rice Husk Extracts on Mild Steel Immersed in 1M H<sub>2</sub>SO<sub>4</sub> and HCl Solutions

K. K. Alaneme<sup>1,2,\*</sup>, Y. S. Daramola<sup>1</sup>, S. J. Olusegun<sup>1</sup>, A. S. Afolabi<sup>3</sup>

<sup>1</sup>Department of Metallurgical and Materials Engineering, Federal University of Technology, Akure, PMB 704, Nigeria

<sup>2</sup>Department of Mining and Metallurgical Engineering, University of Namibia, Faculty of Engineering Campus, Ongwediva, P. O. Box. 3624, Namibia

<sup>3</sup>Department of Civil and Chemical Engineering, University of South Africa, Johannesburg, South Africa

\*E-mail: [kkalaneme@gmail.com](mailto:kkalaneme@gmail.com)

Received: 23 October 2014 / Accepted: 28 December 2014 / Published: 24 February 2015

---

Corrosion inhibition characteristics of extract of rice husk ash on mild steel in 1 M HCl and H<sub>2</sub>SO<sub>4</sub> was investigated in this work. The study was carried out using mass loss, inhibition efficiency, atomic adsorption spectroscopy (AAS), FT-IR spectroscopy and surface analysis as bases for assessing the inhibition and adsorption properties of the extract in the acid solutions. The analyses of the results showed that the inhibition efficiency increased with increase in concentration of the inhibitor and decreased with temperature in both acid solutions. The efficiency of the extract in HCl (96%) was noted to be more than in H<sub>2</sub>SO<sub>4</sub> (86%) solution. Thermodynamic parameters revealed that the adsorption of extract onto the metal surface was spontaneous. FTIR results showed that the inhibition mechanism was by absorption process, through the functional groups present in the extract. The SEM images of the corrosion product confirmed the protection offered by the extract on the surface of the metal immersed in both media. The data obtained were fitted into Langmuir and Freundlich adsorption isotherms though the Langmuir model was found to be better fitted than the Freundlich.

---

**Keywords:** adsorption; corrosion, inhibition; FTIR; mass loss; rice husk

### 1. INTRODUCTION

Corrosion of engineering structures and components in service has continued to be a huge source of concern to corrosion experts in the academia and industries. This is primarily due to its deleterious effect on material integrity and mechanical properties resulting in failure in severe cases

[1]. A study conducted in 2002 estimated an expenditure of 3.1% of GDP as the cost of addressing corrosion related problems by the US economy [2]. Considering the huge cost of corrosion monitoring and control, a great deal of efforts have been channeled towards developing technically efficient and cost-effective strategies for corrosion management [3]. The use of corrosion inhibitors has been very promising in this regards particularly with the use of plant based materials. Plant based inhibitors offer a number of advantages such as biodegradability, absence of heavy metals or other toxic compounds, availability and ease of processing [4].

The inhibition characteristics of a good number of green inhibitors have been studied: researchers have reported the utilization of extract from plants such as *Euphorbia hirta* and *Dialium guineense* [5] *Hyptis Suaveolens* [6] *Water hyacinth* [7] *Sida acuta* [8] *Jatropha Curcas* [9] *Daniella Oliverri* [10] *Tithonia Diversifolia* [11] *Aloes* [12] *Cordia dichotoma* [13]. Their inhibition efficiencies and adaptability for commercial use have been very promising and have raised hope for complete replacement of the more expensive and toxic synthetic inhibitors. Nonetheless, research work is still needed on other potential plant based inhibitors especially those with less medicinal and other competing applications.

In this study, the extract of rice husk was utilized as inhibitor of corrosion on mild steel in HCl and H<sub>2</sub>SO<sub>4</sub> solutions. The choice of rice husk was based on the results obtained from its phytochemical screening which confirms the presence of tannins. It has been established from the literature that plants that contains tannins and flavonoids among others could act as effective corrosion inhibitor [14].

## 2. MATERIALS AND METHODS

### 2.1 Materials

A cylindrical mild steel sample of composition Fe=98.3%, C=0.133%, P=0.0061%, Mn=0.82%, Cr=0.08% was used for this study. The steel was mechanically cut to coupons of dimension 20 x 10 cm, and then polished using different grades of silicon carbide paper, and stored in a moisture-free desiccators prior to use. Analar grade HCl and H<sub>2</sub>SO<sub>4</sub> and distilled water were used for the preparation of the acid solution while rice husks (RH) were used as a source of corrosion inhibitor.

### 2.2 Preparation of rice husk extract

Rice husks were obtained from a rice processing plant at Igbemu-Ekiti, Ekiti State, Nigeria. The husks were gathered, sun dried and pulverized. About 10 g of the pulverized husk was weighed and added to 100 ml of prepared 1 M HCl and H<sub>2</sub>SO<sub>4</sub> solutions in separate reagent bottles. The mixtures were immersed in a water bath maintained at 90°C for 3 hours, after which they were removed from the water bath and allowed to cool overnight. The mixtures were then filtered to obtain the extract. Stock solutions of 0.1, 0.2, 0.3, 0.4, and 0.5 % (v/v) rice husk extract in 1 M HCl and H<sub>2</sub>SO<sub>4</sub> solutions were prepared from the filtrate.

### 2.3 Weight loss measurement

Weight loss studies were carried out on pre-weighed mild steel samples which were immersed in 250 ml capacity beakers containing 100 ml of the test solutions maintained at 303, 313, 323 and 333 K in a thermostat controlled water bath. The substrates were held in the solutions for 4 hours after which they are reweighed and the difference in weight taken as weight loss. From the weight loss data obtained, the corrosion rates (CR), inhibition efficiency (IE) and surface coverage ( $\Theta$ ) were calculated using equations (i) – (iii) respectively:

$$\text{CR (mgh}^{-1}\text{cm}^{-2}\text{)} = \frac{\Delta W}{AT} \quad (\text{i})$$

where,  $\Delta W$  is weight loss, A is the area of the coupon in  $\text{cm}^2$  and T is time in hour.

$$\text{IE \%} = \left(1 - \frac{\text{CR}_{\text{inh}}}{\text{CR}_{\text{blank}}}\right) \times 100 \quad (\text{ii})$$

where  $\text{CR}_{\text{inh}}$  and  $\text{CR}_{\text{blank}}$  correspond to the corrosion rates in the blank and inhibitor solutions respectively, and the surface coverage calculated using:

$$\Theta = \left(1 - \frac{\text{CR}_{\text{inh}}}{\text{CR}_{\text{blank}}}\right) \quad (\text{iii})$$

### 2.4 Mass loss measurement

Pre-weighed mild steel samples were immersed in 100 ml of the blank/inhibitor solutions for 7 days (168 hours). The weight loss of each coupon was determined at every 24 hour intervals by retrieving the samples from the solution, cleaned with acetone and then reweighed. The mass loss for each sample was evaluated by dividing its weight loss by the surface area of the coupon [11].

### 2.5 Atomic adsorption spectrometric analysis

Atomic adsorption analysis was performed using atomic adsorption spectrometer model bulk 200. This was required to determine the concentration of iron (II) ions in the acidic solutions after gravimetric measurements. The calibration curve of iron (II) ions was drawn before analyzing the electrolyte solution. All samples containing iron ions were diluted with distilled water to ensure that the concentrations of metal ions are within the range of the calibration curve.

### 2.6 FTIR analysis

FTIR analysis was carried out to determine the functional groups present in the RH extract and that of the corrosion products from the mild steel corrosion set ups containing the RH extract were carried out using Perkin-Elmer-1600 Fourier transform infra-red spectrophotometer. The samples were prepared for the analysis using KBr.

### 2.7 Scanning electron microscopy and energy dispersive spectroscopy (SEM-EDS) analyses

The surface morphology of the mild steel before and after immersion in the corrosion media, and the elemental composition of the metal surfaces were examined using a JSM 7600F Jeol ultra-high

resolution field emission gun scanning electron microscope (FEG-SEM) equipped with accessories for energy dispersive spectroscopy.

### 3. RESULT AND DISCUSSION

#### 3.1 Phytochemical screening

The phytochemical constituents of the extracts as presented in Table 1, shows the presence of tannins, saponins among others. The presence of these compounds has been reported to promote the inhibition of mild steel in aggressive acidic media [15].

**Table 1.** Phytochemical constituents of rice husk extract

Phytochemical constituents	Saponins	Tannins	Flavonoids	Legal Test	Keller Killani
R-HCl	-	+	+	+	+
R-H <sub>2</sub> SO <sub>4</sub>	-	+	+	+	+

#### 3.2 FTIR analysis of the extract and corrosion product

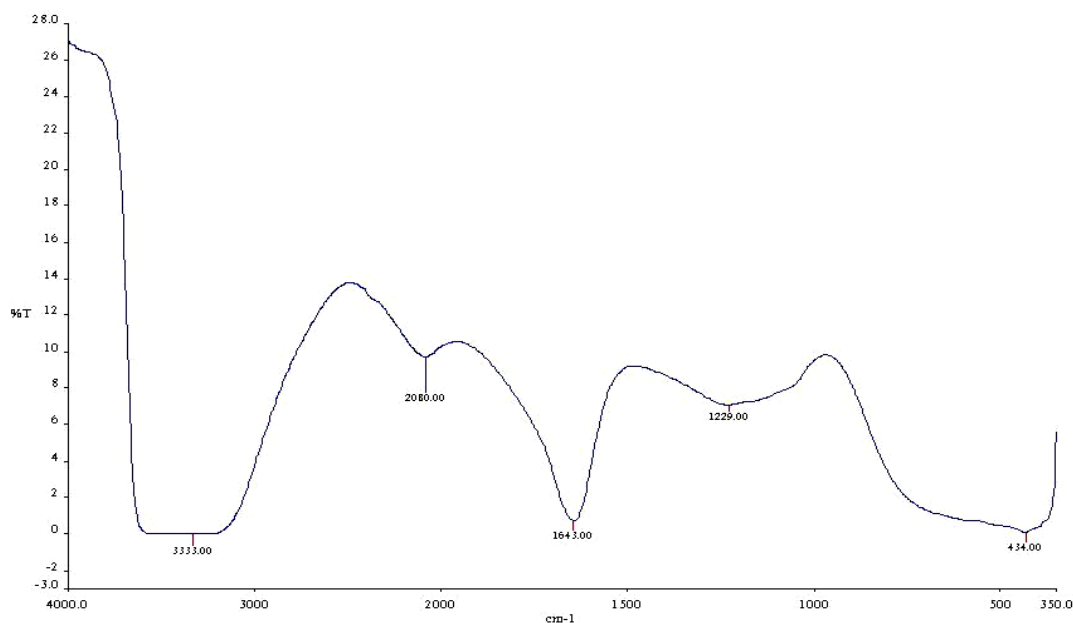


**Figure 1.** IR spectrum of HCl extract of RH

Presented in Figures 1 – 4 show the FTIR spectra of the RH extract and the corrosion product. It can be seen that the IR spectra of the rice husk extracts from HCl and H<sub>2</sub>SO<sub>4</sub> solutions (Figures 1 and 2) show similar bands. The broad band obtained at 3333 and 3396 can be assigned to OH. The frequency at 2080 and 2102.85 corresponds to C-H stretching, and the one at 1643.84 cm<sup>-1</sup>

corresponds to C=C. Comparing the spectra of the rice husk extracts from both acidic media with that of the solid corrosion product (Figures 3 and 4), it is observed that there are shifts in the frequencies. The shifts in the spectra indicate that the interaction between the extracts and mild steel occurred through the functional groups presents in them. Moreover, it can be affirmed that the functional group has coordinated with  $Fe^{2+}$  formed on the metal surface resulting in the formation of  $Fe^{2+}$  extract complex on the metal surface, which promotes the inhibition of the metal sample.

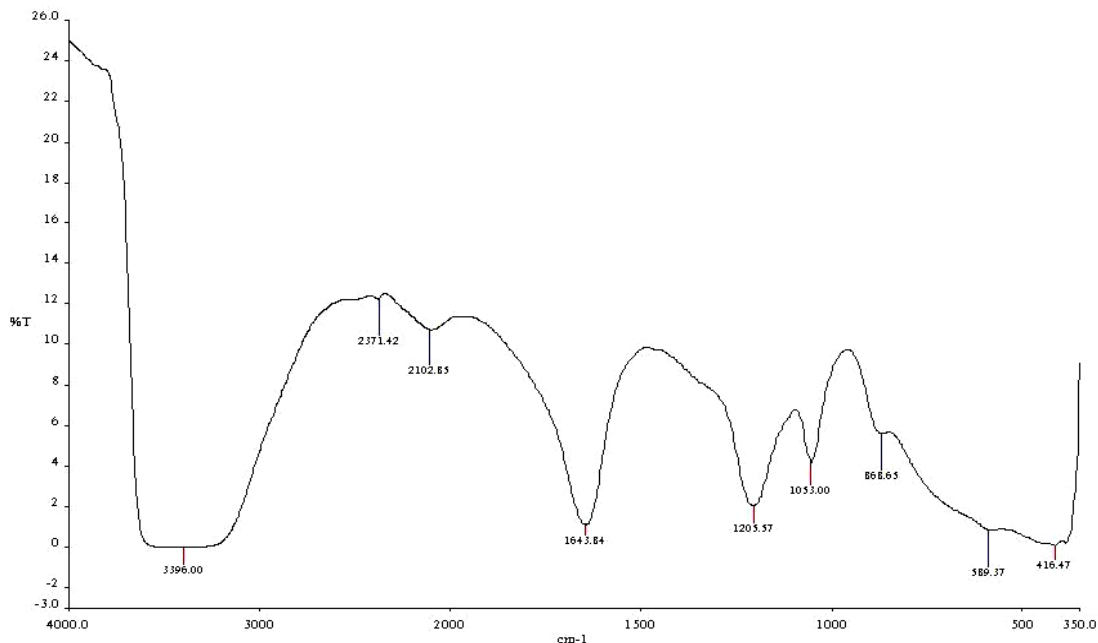


**Figure 2.** IR spectrum of  $H_2SO_4$  extract of RH

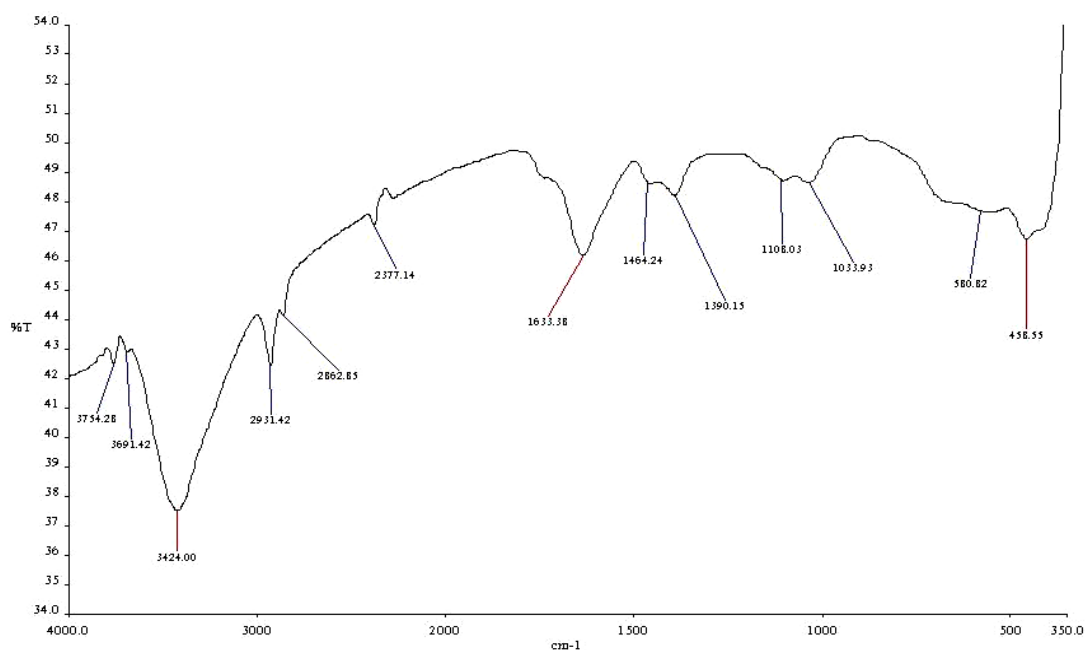


**Figure 3.** IR spectrum of solid corrosion product in the HCl extract of RH

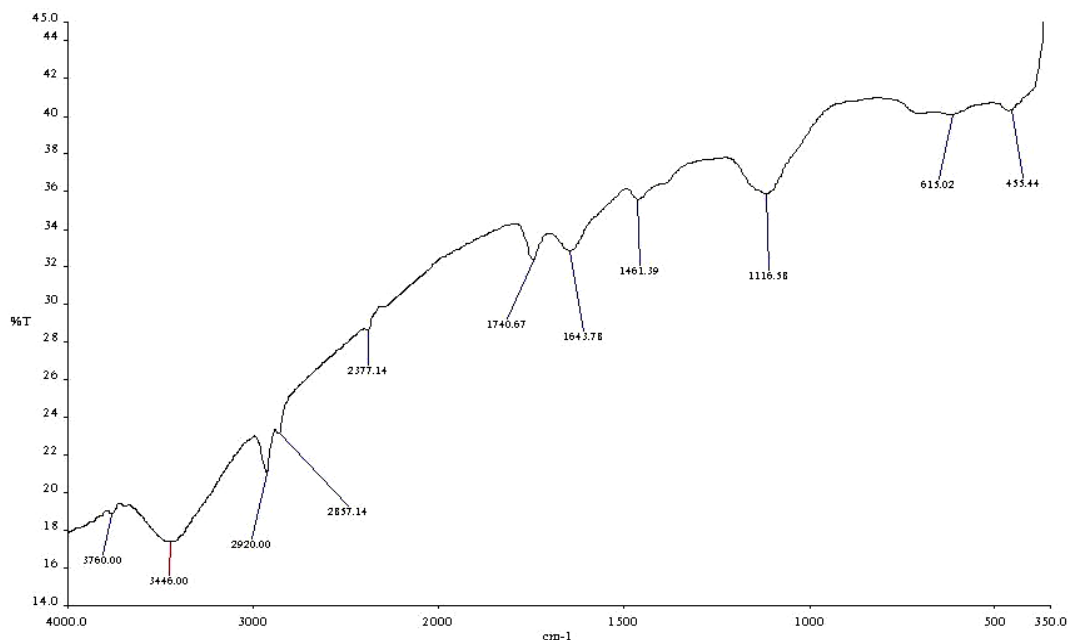


**Figure 4.** IR spectrum of solid corrosion product in the  $\text{H}_2\text{SO}_4$  extract of RH

### 3.3 Mass loss measurement

The variation of mass loss in the absence and presence of the rice husk extracts from HCl and  $\text{H}_2\text{SO}_4$  Solutions are presented in Figure 5. It can be observed from the Figure that the mass loss increased with increase in exposure time. Also, the addition of rice husk extract from HCl solution resulted in a significant reduction in the mass loss of the mild steel substrate in comparison with the blank solution. The rice husk extract from  $\text{H}_2\text{SO}_4$  solution on the other hand could not reduce the mass loss significantly as that of rice husk extract from HCl solution. Ehteram [16] suggested the mechanism that would have led to the performance of RHCl than  $\text{RH}_2\text{SO}_4$ , he noted that the acid's anions of acids ( $\text{Cl}^-$  or  $\text{SO}_4^{2-}$ ) adsorb physically on the positively charged metal surface, giving rise to a net negative charge on the metal surface. Then the organic cations are physically attracted to the anions layer which is formed on the metal surface. According to the ionic volume of the acid's anions the smallest anion ( $\text{Cl}^-$ ) attracted faster to the metal surface than the biggest one ( $\text{SO}_4^{2-}$ ) leading to good inhibitor performance in HCl. The reduction in mass loss in the presence of the extract has been attributed to the adsorption of phytochemical constituents (Table 1) which are present in the extract. Saratha and Vasudha [17] opined that the adsorption of such compounds on the metal surface creates a barrier for charge and mass transfer leading to a decrease in the interaction between the metal and the corrosive environment.

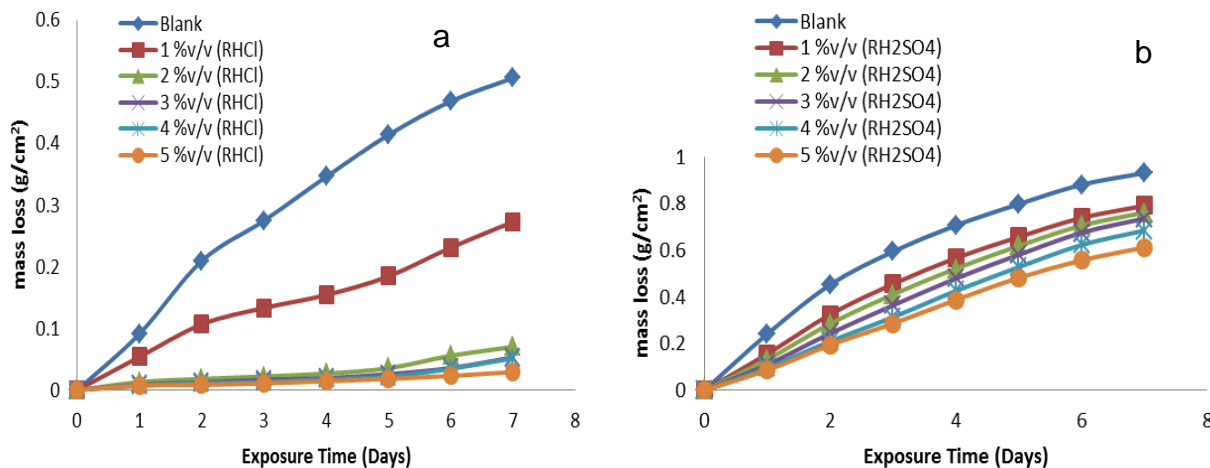


**Figure 5.** Variation of mass loss with rice husk (a) HCl and (b) H<sub>2</sub>SO<sub>4</sub> acid extracts as a function of time

The plots of the dissolution of Fe<sup>2+</sup> in the electrolyte (obtained from AAS analysis) as function of the extract concentration are shown in Figure 6. These plots serve as a confirmatory test to what was obtained from the mass loss measurement. It is seen that there is a steady decrease in the concentration of Fe<sup>2+</sup> in the electrolyte as more extracts are added. This indicates that the adsorption of the extract on the metal surface reduced the oxidation of iron atom Fe to Fe<sup>2+</sup>.

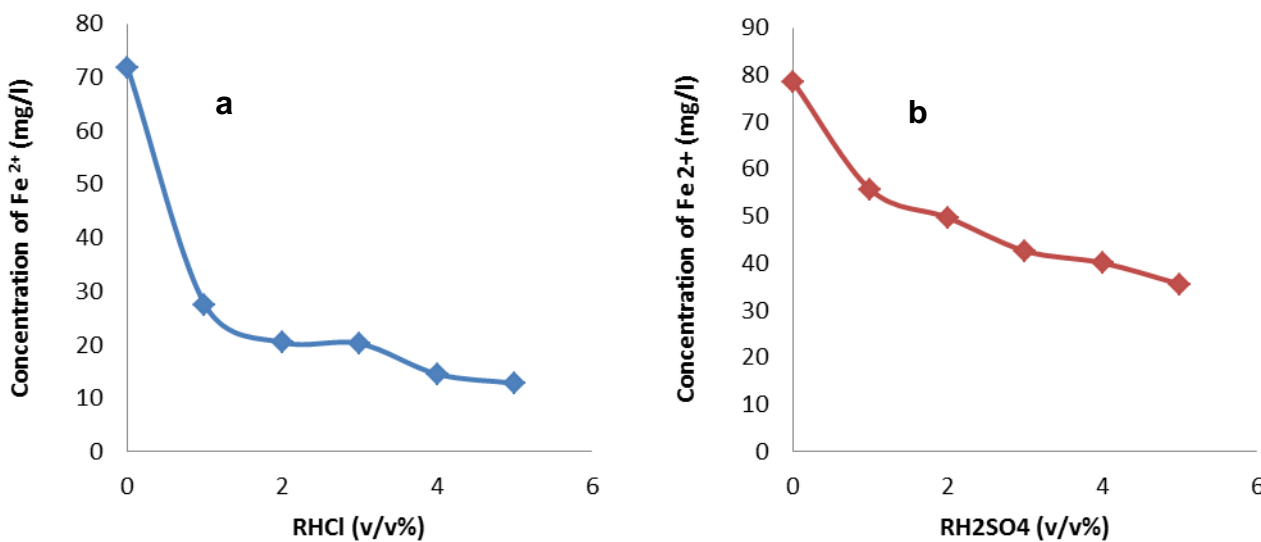


**Figure 6.** Plots of the concentrations of iron (II) ions in 1 M (a) HCl and (b) H<sub>2</sub>SO<sub>4</sub> acids after gravimetric measurements

### 3.4 Effect of temperature on the inhibition efficiency and corrosion rate

The variations of inhibition efficiencies (IE) with temperature for the mild steel substrates in HCl and H<sub>2</sub>SO<sub>4</sub> solutions with and without the rice husk extract from both acidic solutions are

presented in Figure 7. From the Figure (a and b), it is observed that on the average the inhibition efficiencies of the HCl solution containing HCl extract of rice husk is generally higher than the H<sub>2</sub>SO<sub>4</sub> solution containing H<sub>2</sub>SO<sub>4</sub> extract of rice husk. It can also be observed that the inhibition efficiency decreases with increase in temperature for both acidic media. Ambrish et al [18] attributed this behavior to increased rate of dissolution process of mild steel and partial desorption of the inhibitor from the metal surface with higher temperature. However, in H<sub>2</sub>SO<sub>4</sub> solution the inhibition efficiency values are more sensitive to the extract concentration as reflected by the significant increases in inhibition efficiencies in comparison to the HCl solution where there are marginal changes in the inhibition efficiencies with increase in the extract concentration.

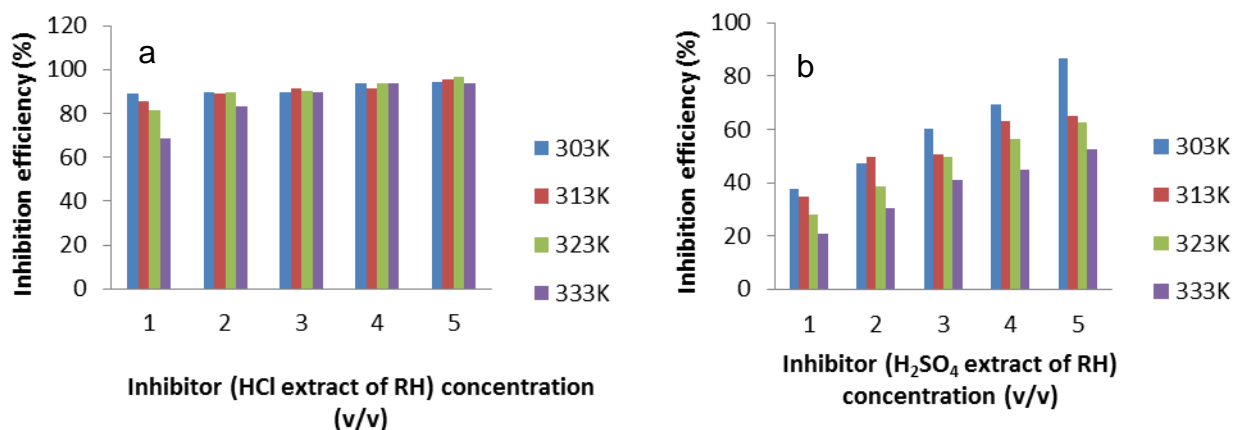


**Figure 7.** Variation of inhibition efficiency of (a) HCl and (b) H<sub>2</sub>SO<sub>4</sub> extracts of RH with concentration at 303 – 333K.

**Table 2.** Corrosion rates (CR) of mild steel in HCl and H<sub>2</sub>SO<sub>4</sub> in the absence or presence of RH extract

Acid medium	Concentration of HCl extract RH of (% v/v)	Corrosion rate (mg cm <sup>-2</sup> h <sup>-1</sup> )			
		303K	313K	323K	333k
1 M HCl	Blank	10.42	18.20	24.82	35.20
	1	1.12	2.60	4.63	10.96
	2	1.09	2.00	2.80	5.81
	3	1.06	1.57	2.38	3.63
	4	0.65	1.53	1.62	2.136
	5	0.56	0.80	1.52	2.11
Acid medium	Concentration of H <sub>2</sub> SO <sub>4</sub> extract RH of (% v/v)	Corrosion rate (mg cm <sup>-2</sup> h <sup>-1</sup> )			
		303K	313K	323K	333k
1 M H <sub>2</sub> SO <sub>4</sub>	Blank	13.50	19.98	33.58	53.52
	1	8.40	13.00	24.22	42.28
	2	7.13	10.94	20.61	37.29
	3	5.37	9.90	16.86	31.61
	4	4.12	7.41	14.65	29.50
	5	1.77	6.94	12.60	25.46



Table 2 shows the values of corrosion rate at different temperatures and concentrations of the extract. From the Table, corrosion rate in both the absence and presence of the extracts increases with increase in temperature. This result is expected because as the temperature increases the average kinetic energy of the reacting molecules increases thereby speeding up the reaction rate [19]. Nonetheless, the corrosion rate values decrease with increase in the concentration of the extract.

### 3.5 Apparent activation energy of metal dissolution process

The corrosion rate values obtained in Table 1 were used to evaluate the activation energy using equation (iv). A plot of log of corrosion rate (CR) obtained from gravimetric measurement against 1/T produced a straight line in both absence and presence of the extracts as shown in Figure 8

$$\log CR = \log A - \frac{E_a}{2.303RT} \tag{vi}$$

where CR is the corrosion rate,  $E_a$  is the apparent activation energy,  $R$  is the molar gas constant,  $T$  is the absolute temperature and  $A$  is the frequency factor.

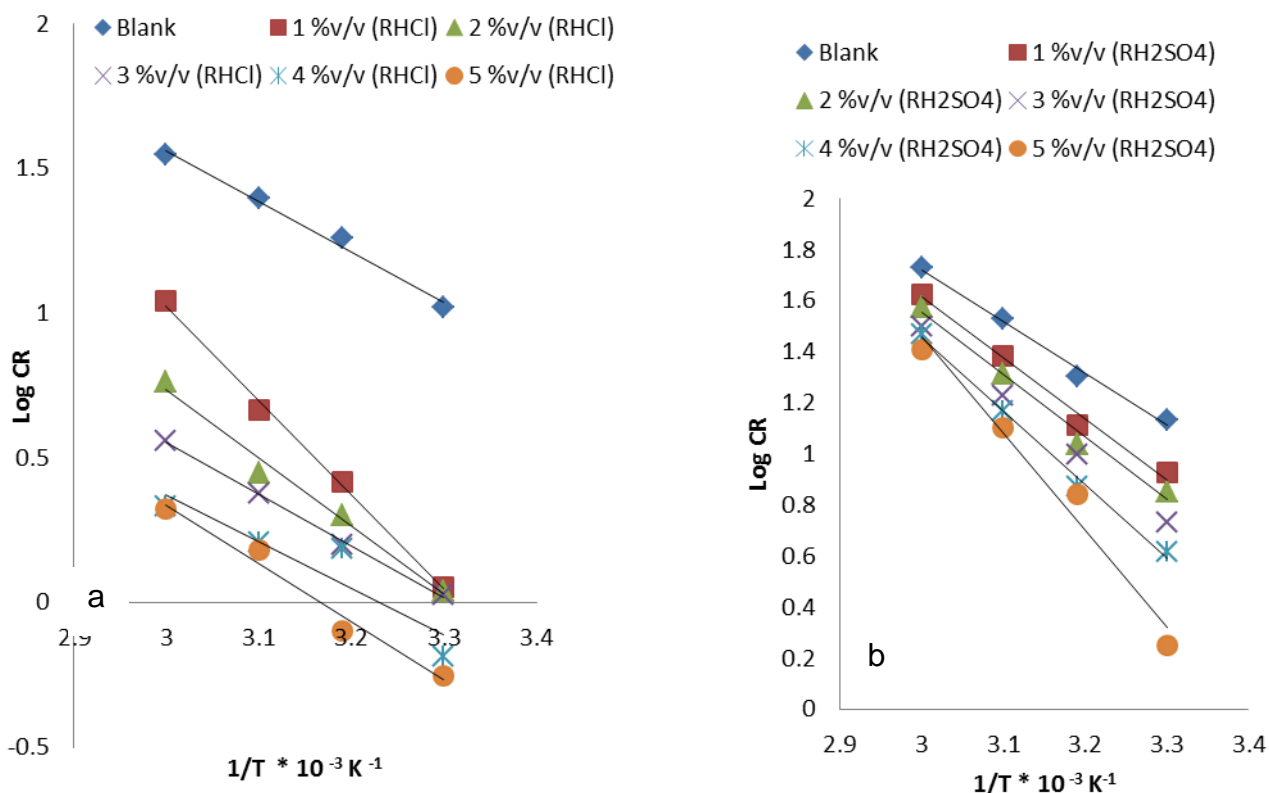


**Figure 8.** Arrhenius plot for mild steel corrosion in (a) HCl and (b) H<sub>2</sub>SO<sub>4</sub> extracts of RH with concentration at 303 – 333 K.

The values of activation energy obtained from the slope ( $-E_a/2.303R$ ) are presented in Table 3 from which it is observed that the  $E_a$  values obtained in the presence of the extracts are higher than in the absence except at 4% (v/v) concentration in 1 M HCl. Similar trends from was been used to establish that when the  $E_a$  increases in the presence of inhibitor such a reaction process is interpreted

as physical adsorption [20]. This then denotes that the phytochemical constituents in the extracts are weakly bonded or adsorbed on the mild steel surface.

The activation energy in the absence of the extracts is 33.38 and 38.93 kJ/mol in 1 M HCl and H<sub>2</sub>SO<sub>4</sub> respectively. They are lower than the values obtained in the presence of inhibitor. The values in the presence of the HCl and H<sub>2</sub>SO<sub>4</sub> extract of RH ranged from 30.90 to 62.23 (mean = 42.26 kJ/mol) and 45.74 to 72.48 kJ/mol (mean = 53.84 J/mol) respectively.

### 3.6 Enthalpy ( $\Delta H_a$ ) and entropy ( $\Delta S_a$ ) of metal dissolution process

The enthalpy ( $\Delta H_a$ ) and entropy ( $\Delta S_a$ ) of activation of corrosion process were calculated from an alternative formulation of Arrhenius equation [21].

$$\log \frac{CR}{T} = \log \left( \frac{R}{nh} \right) + \frac{\Delta S_a}{2.303R} - \frac{\Delta H_a}{2.303RT} \tag{v}$$

where CR is the corrosion rate at Temperature  $T$ ,  $R$  is the molar gas constant,  $n$  is Avogadro’s constant, and  $h$  is the Planck’s constant. A plot of  $\log \frac{CR}{T}$  versus  $1/T$  produces a straight line (Figure 9) with a slope of  $(-\Delta H_a/2.303R)$  and an intercept of  $(\log(R/nh) + \Delta S_a/2.303R)$  from which the values of  $\Delta H_a$  and  $\Delta S_a$  were calculated and presented in Table 3.

**Table 3.** Activation energy, enthalpy and entropy parameters of the mild steel dissolution in HCl and H<sub>2</sub>SO<sub>4</sub> in the presence and absence of RH at temperature range of 303–333 K

Acid medium	Concentration of HCl extract RH of (% v/v)	Activation energy, $E_a$ (kJ mol <sup>-1</sup> )	Enthalpy of activation, $\Delta H_a$ (kJ mol <sup>-1</sup> )	Entropy of activation, $\Delta S_a$ (J mol <sup>-1</sup> k <sup>-1</sup> )
1 M HCl	Blank	33.38	30.73	-123.78
	1	62.23	59.59	-47.53
	2	44.91	41.67	-107.06
	3	34.44	31.80	-139.86
	4	30.90	28.26	-153.99
	5	38.65	30.61	-149.80
Acid medium	Concentration of H <sub>2</sub> SO <sub>4</sub> extract RH of (% v/v)	Activation energy, $E_a$ (kJ mol <sup>-1</sup> )	Enthalpy of activation, $\Delta H_a$ (kJ mol <sup>-1</sup> )	Entropy of activation, $\Delta S_a$ (J mol <sup>-1</sup> k <sup>-1</sup> )
1 M H <sub>2</sub> SO <sub>4</sub>	Blank	38.93	36.29	-104.06
	1	45.74	35.22	-109.85
	2	46.80	44.78	-81.87
	3	49.05	46.41	-78.10
	4	55.14	52.50	-60.54
	5	72.48	69.84	-8.43

The results show that the enthalpy of activation values are all positive, which reflects the endothermic nature of the mild steel dissolution process. Moreover, the enthalpy of activation in the presence of the extracts is more than in the blank solution. This indicates that mild steel dissolution requires more energy in the presence of the extract than in the absence.

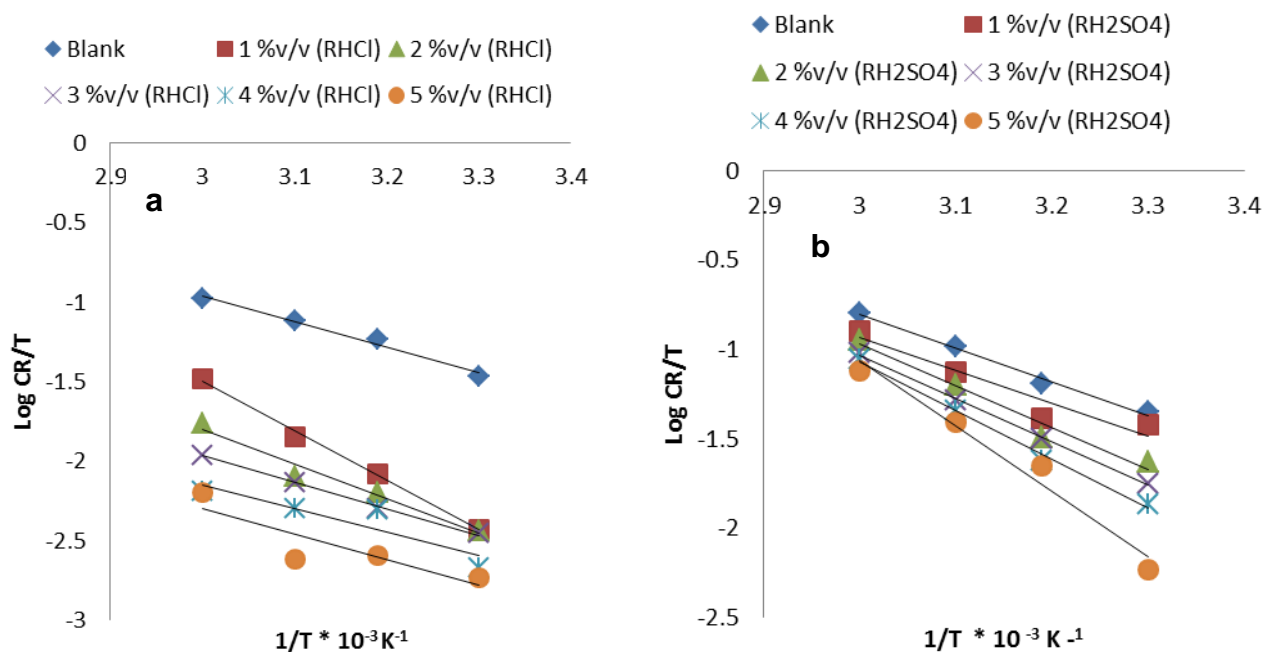


**Figure 9.** Transition state plots for mild steel corrosion in (a) HCl and (b) H<sub>2</sub>SO<sub>4</sub> extracts of RH with concentration at 303 – 333 K.

### 3.7 Adsorption isotherm

The Langmuir adsorption isotherm was applied to investigate the mechanism of the corrosion inhibition by using equation (vi):

$$\frac{C}{\theta} = \frac{1}{K_{ads}} + C \tag{vi}$$

where C is the inhibitor concentration,  $\theta$  (IE/100) is the surface coverage and  $k_{ads}$  is the adsorption equilibrium constant which  $K_{ads}$  denotes the strength between adsorbate and adsorbent [22]. The plot of  $C/\theta$  versus C is linear as shown in Figure 10 indicating that the adsorption of the inhibitor on the surface of mild steel is consistent with Langmuir isotherm and the slopes obtained are unity.

The correlation coefficient ( $R^2$ ) of the adsorption isotherm data shows that Langmuir isotherm is best fitted into the experiment with  $R^2$  ranges from 0.9992 - 0.9997 and 0.9424 – 0.9934 for HCl and H<sub>2</sub>SO<sub>4</sub> extract of RH respectively, at temperatures studied.

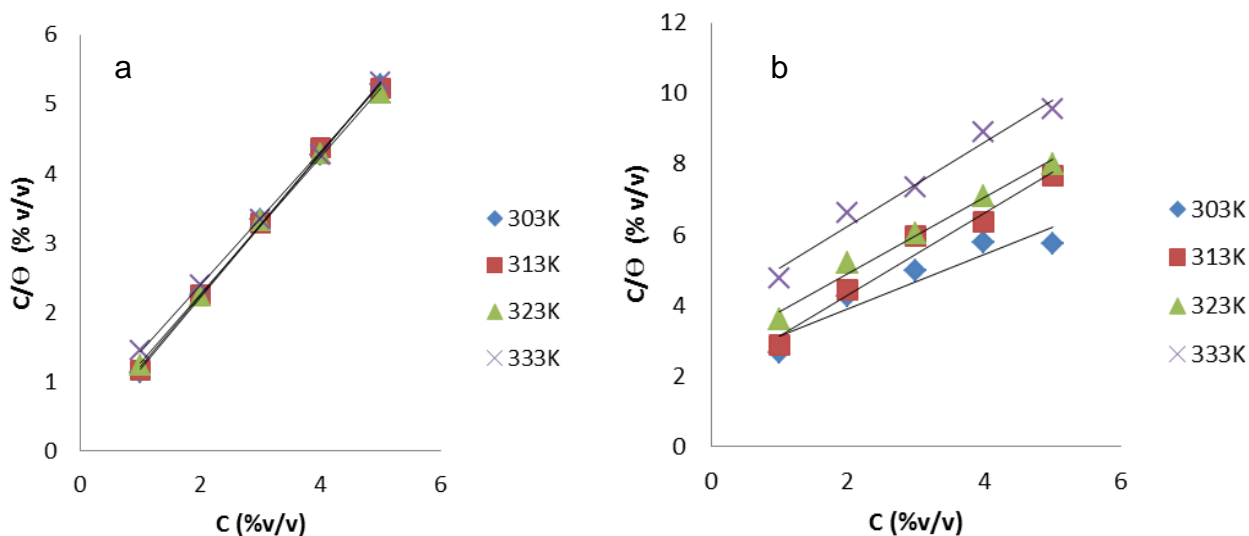


**Figure 10.** Langmuir adsorption isotherm plots for the adsorption of (a) HCl and (B) H<sub>2</sub>SO<sub>4</sub> extracts of RH with concentration at 303 – 333 K.

The values of correlation coefficient ( $R^2$ ) and adsorption coefficient ( $K_{ads}$ ) are presented in Table 4. The values of  $K_{ads}$  show that adsorption coefficient decreases with increase in temperature. Similar result was also reported by [23]. This is an indication that the inhibition efficiency decreases with temperature.

**Table 4.** Langmuir isotherms parameter

Temperature	Concentration of HCl extract RH of (% v/v)			Concentration of H <sub>2</sub> SO <sub>4</sub> extract RH of (% v/v)		
	$R^2$	$K_{ads}$	Slope	$R^2$	$K_{ads}$	Slope
303K	0.9993	7.03	1.03	0.9424	0.423	0.77
313K	0.9992	5.40	1.02	0.9848	0.503	1.15
323K	0.9993	3.67	0.99	0.9934	0.363	1.07
333K	0.9996	2.10	0.95	0.9867	0.258	1.18

### 3.8 SEM analysis

The SEM micrographs of the mild steel before and after immersion in HCl and H<sub>2</sub>SO<sub>4</sub> in the absence and presence of the rice husk extract are presented in Figures 11 – 13. The surface morphologies served as a good indicator of the severity of corrosion attack.

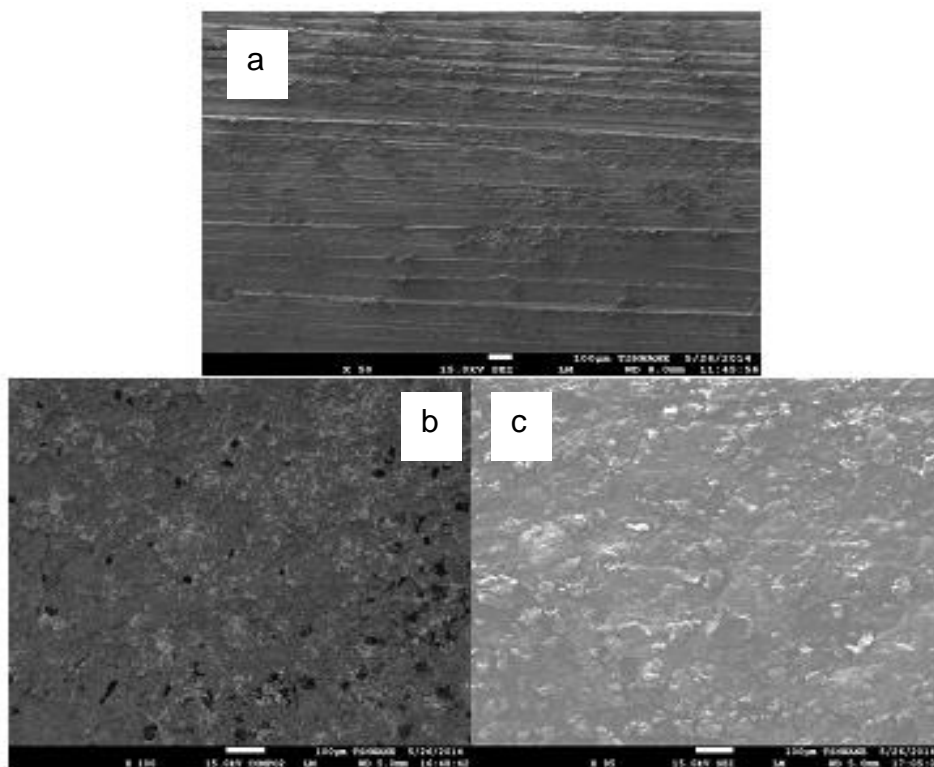


**Figure 12.** SEM images of the mild steel (a) before immersion, after immersion in the (b) blank and (c) extract solutions of HCl

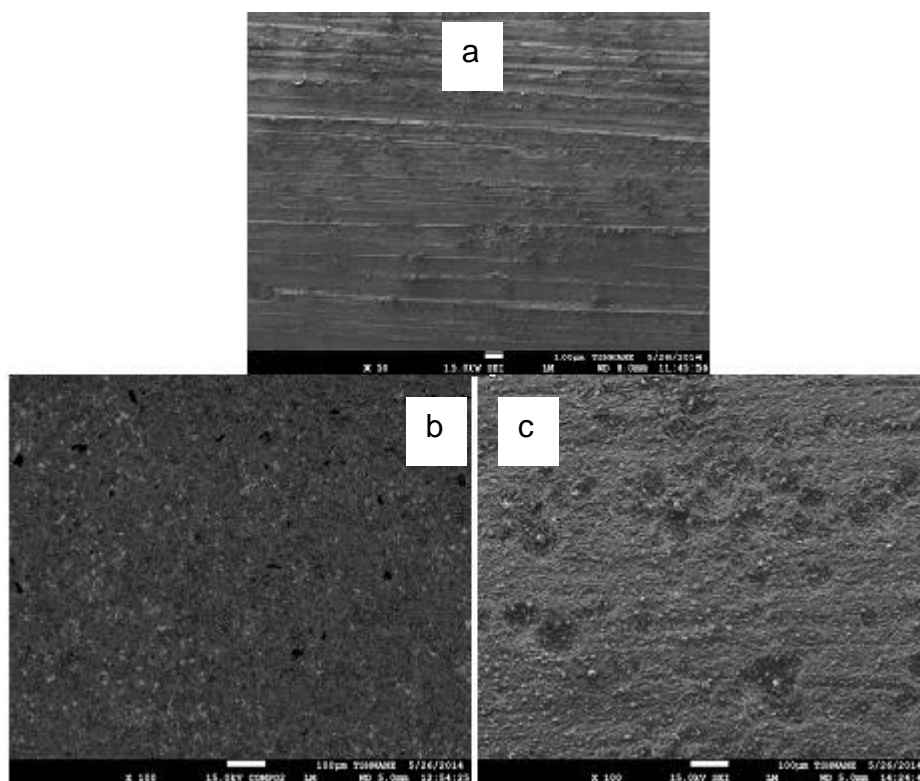


**Figure 13.** SEM images of the mild steel (a) before immersion, after immersion in the (b) blank and (c) extract solutions of H<sub>2</sub>SO<sub>4</sub>

It can be noticed from the micrographs that the substrates immersed in the acidic media without the extract had more pronounced depth of pitting (Figures 12a and 13a) compared to the substrates which contained the rice husk acid extracts (Figures 12b and 13b).

#### 4. CONCLUSIONS

This study investigated the properties of corrosion inhibition of extract of rice husk ash on mild steel in 1 M HCl and H<sub>2</sub>SO<sub>4</sub> using the conventional gravimetric measurements. The analyses of the results showed that the inhibition efficiency increased with increase in concentration of the inhibitor but decreased with temperature in both acid solutions. The physical adsorption mechanism of the inhibition process was in conformation with the data obtained, and Langmuir and Freundlich models were best fitted into the obtained results. The calculated activation energy values also conformed to a physical adsorption mechanism. The SEM images of the mild steel samples showed that the metal was protected in the presence of the extracts.

#### References

1. Z. Ahmad, *Principles of Corrosion Engineering and Corrosion Control*, Butterworth-Heinemann, Oxford (2006).
2. B. Rapp, *Corrosion, a study of degradation*, Materials today, 9(3) (2006), DOI: 10.1016/S1369-7021(06)71371-2.
3. E. E. Ebenso, *Bulletin of Electrochemistry*, 19(5) (2003) 209.
4. N. O. Eddy, E. E. Ebenso, *African Journal of Pure and Applied Chemistry*, 2(6) (2008) 1.
5. I. U. Anozie, C. S. Akoma, L. A. Nnanna, *International Journal of Pure and Applied Sciences and Technology*, 6(2) (2011) 79.
6. P. Muthukrishnan, B. Jeyaprabha, P. Prakash, *International Journal of Industrial Chemistry*, (2014) 5:5DOI 10.1007/s40090-014-0005-9
7. D. T. Oloruntoba, J. A. Abbas, S. J. Olusegun, Water hyacinth (eichhornia crassipes) leaves extract as corrosion inhibitor for AISI 1030 steel in sea water In: Laryea, S., Agyepong, S.A., Leiringer, R. and Hughes, W. (Eds), *Proceedings of 4th West Africa Built Environment Research (WABER) Conference*, 24-26 July 2012, Abuja, Nigeria, 1131.
8. U.M. Eduok, S.A. Umoren, A.P. Udoh, *Arabian Journal of Chemistry*, 5(2012) 325.
9. S.J. Olusegun, B. A. Adeiza, K. I. Ikeke, M.O. Bodunrin, *Journal of Emerging Trends in Engineering and Applied Sciences*, 4 (2013) 138.
10. N. O. Eddy, A. O. Odiongenyi, P. O. Ameh, E. E. Ebenso, *International Journal of Electrochemical. Science*, 7 (2012) 7425.
11. K. K. Alaneme, S. J. Olusegun, *Leonardo Journal of Sciences*, 20 (2012) 59.
12. H. Cang, Z. Fei, J. Shao, W. Shi, Q. Xu, *International Journal of Electrochemical. Science*, 8 (2013) 720.
13. R. Khandelwal, S.K.Arora, R. K. Upadhyay, S.P. Mathur, R. Parashar, *International Journal of Current Trends in Science and Technology*, 3(2) (2012) 70.
14. B. E. Amitha Rani, Bharathi Bai J. Basu, *International Journal of Corrosion (Hindawi)*, (2012) 1, Doi:10.1155/2012/380217
15. N. O. Eddy, E. E. Ebenso, *African Journal of Pure and Applied Chemistry*, 2(6) (2008) 1.
16. E. A. Noor, *Materials Chemistry and Physics*, 114 (2009) 533.
17. R. Saratha, V. G. Vasudha, *E-Journal of Chemistry*, 7(3) (2010) 677.

18. A. Singh, V. K. Singh, M. A. Quraishi, *Journal of Materials and Environmental Science*, 1 (3) (2010) 162.
19. E. F. Olasehinde, S. J. Olusegun, A. S. Adesina, S. A. Omogbehin, H. Momoh-Yahayah, *Nature and Science*, 11 (2013) 83.
20. J.T. Nwabanne, V.N. Okafor, *Journal of Emerging Trends in Engineering and Applied Sciences (JETEAS)*, 2 (4) (2011) 619.
21. A. S. Fouda, H. Tawfik, A. H. Badr, *Advances in Materials and Corrosion*, 1 (2012) 1.
22. E. I. Ating, S. A. Umoren, I. I. Udousoro, E. E. Ebenso, A. P. Udoh, *Green Chemistry Letters and Reviews*, 3(2) (2010) 61.
23. E. E. Ebenso, N. O. Eddy, A. O. Odiongenyi, *African Journal of Pure and Applied Chemistry*, 2 (11) (2008) 107.

© 2015 The Authors. Published by ESG ([www.electrochemsci.org](http://www.electrochemsci.org)). This article is an open access article distributed under the terms and conditions of the Creative Commons Attribution license (<http://creativecommons.org/licenses/by/4.0/>).